journal

J. Am. Ceram. Soc., 78 [4] 1083–86 (1995)

Hertzian Contact Damage in Magnesia-Partially-Stabilized Zirconia

Antonia Pajares,† Fernando Guiberteau,*,† and Brian R. Lawn*

Materials Science and Engineering Laboratory, National Institute of Standards and Technology, Gaithersburg, Maryland 20899

Srinivasarao Lathabai*

CSIRO Division of Materials Science and Technology, Clayton, VIC 3169, Australia

Hertzian contact damage in magnesia-partially-stabilized zirconia is examined. Ceramographic techniques and acoustic emission reveal the damage patterns to be fundamentally different in the as-fired, peak-aged, and over-aged states. Indentation stress–strain curves show that the plasticity component of the contact deformation increases monotonically with aging time. Whereas the tetragonal–monoclinic transformation plays an important role in the peak-aged material, alternative deformation processes dominate in the other states: microcracking in as-fired, and monoclinic twinning in over-aged.

I. Introduction

ZIRCONIA-BASED materials, specifically magnesia-partially-stabilized zirconia (Mg-PSZ), can be substantially toughened by phase transformation.[1–3] For a given zirconia, the usually quoted "toughness" is the plateau value on a rising *R*-curve. These long-crack toughness values initially increase with aging time to a peak value, and then decline, corresponding to an optimal state for transformation of tetragonal particles into the monoclinic phase within the crack-tip stress field. This trend translates in some measure to an optimization in strength properties.[2,4]

However, long-crack toughness data do not always pertain to events at the grain scale, where properties like microfracture-assisted wear are often determined. In alumina, for example, increasing grain size increases the long-crack toughness but simultaneously diminishes the short-crack toughness,[5] correspondingly reducing the wear resistance in severe abrasion conditions.[6,7] Despite the intense research activity in zirconia-based ceramics during the last 20 years,[1,2,8–11] very little attention has been given to short-crack phenomena in these materials.[12]

It is in this context that recent developments in Hertzian tests using spherical indenters offer new insights.[13,14] Radical departures from the classical cone crack patterns that characterize such homogeneous brittle materials as glasses and single crystals[15,16] and ultra-fine-grain polycrystal ceramics[17,18] are observed in several heterogeneous, toughened ceramics.[14,19–23] In the latter materials, cone fracture is partially or fully suppressed in favor of distributed, microstructurally localized damage in a zone of high compression–shear beneath the contact circle. Macroscopically, the shape of the damage zone resembles that observed in metals,[24] and may accordingly be regarded as a kind of "plasticity" or "quasi-ductility." Evolution of the plastic component of the deformation is readily quantified as a departure from ideal linear elastic on an indentation stress–strain curve.[14,19,20]

The present study investigates the nature of Hertzian contact damage in a Mg-PSZ material, in the as-fired (AF), peak-aged (PA), and over-aged (OA) states. We will find that the mode of damage is fundamentally different for the material in each of these three aging states. Whereas the tetragonal–monoclinic transformation plays an important role in the PA material, alternative deformation processes dominate in the other states.

II. Experimental Procedure

Eutectoid-aged 9.9 mol% Mg-PSZ (ICI Advanced Ceramics, Australia), as previously described,[4] was used in this study. The fabrication process involved an initial sintering in the cubic (*c*) phase field at a temperature ≈1700°C, followed by cooling at ≈500°C/h, producing an AF material with finely dispersed intragranular tetragonal (*t*) precipitates. This particular sintering cycle was chosen so that none of the precipitates were coarse enough to effect transformation to the monoclinic (*m*) phase, thus providing an untoughened material for baseline comparison. Some specimens were then heat-treated at the eutectoid temperature of 1400°C to coarsen the precipitates: for 2 h, producing PA specimens with optimum strength; and for 16 h, producing OA specimens with diminished strength (although not back to the low level of the AF material).

Microstructures have been previously characterized by optical and electron microscopy and neutron diffraction, to establish the *c*-phase matrix grain structure and sizes and relative proportions of the *t* and *m* precipitates.[4] During the aging the size of the matrix grains remains invariant at ≈35 μm, but the precipitates coarsen at the expense of the cubic phase and ultimately transform spontaneously above a critical size. In the AF state, the phases are in the ratio $c/t/m \approx 80/20/0$, with subcritical lenticular precipitates ≈100 nm in length. In PA, the ratio is $c/t/m \approx 55/45/0$, with near-critical precipitates ≈300 nm. In OA, the ratio is $c/t/m \approx 50/10/40$, with supercritical precipitates ≈500 nm.

Specimens from each aging state were polished to 1-μm finish with diamond paste, and gold coated prior to indentation. Indentations were made using tungsten carbide (WC) spheres of radius r = 1.59, 1.98, 3.18, 4.76, 7.94, and 12.7 mm in a universal testing machine (Model 1122, Instron, Canton, MA) at constant crosshead speed 1.67 $\mu m \cdot s^{-1}$, with peak indentation loads P = 600, 1000, 1500, 2000, 2500, and 3000 N. The surface contact radius a was determined from the residual impression left in the gold coating at each prescribed peak load P,[13] to enable evaluation of the indentation stress ($p_0 = P/\pi a^2$) as a function of indentation strain (a/r).[25–27]

Optical microscopy of the *surface* damage was carried out on specimens coated after rather than before indentation. For *subsurface* damage, tests were made on bonded-interface specimens.[19,20] Two polished half-blocks were bonded with a thin

D. Shetty—contributing editor

Manuscript No. 193042. Received November 16, 1994; approved February 2, 1995.
Supported by the U.S. Air Force Office of Scientific Research. Additional support for A. Pajares was provided by the Ministerio de Educación y Ciencia (DGICYT); additional support for F. Guiberteau was provided by the Junta de Extremadura, Spain.
*Member, American Ceramic Society.
†Guest Scientist from the Departamento de Fisica, Universidad de Extremadura, 06071 Badajoz, Spain.

layer (<5 μm) of adhesive (Loctite, Newington, CT) to form a vertical internal interface, and the top horizontal surface was then ground and polished. A sequence of indentations was subsequently made along the interface trace on the top surface. The two halves of the indented specimen were then separated by dissolving the adhesive in acetone. The top and side faces were gold coated and examined in Nomarski interference contrast to provide surface and subsurface views of the damage patterns. Some scanning electron microscope examinations were also made on the sections for fine detail.

Acoustic emission was used to monitor the damage evolution during indentation (LOCAN 320, Physical Acoustics, Princeton, NJ). Acoustic activity was recorded using a piezoelectric transducer attached with rubber cement to the specimen top surface. Data were recorded as accumulated acoustic energy vs elapsed time at constant crosshead displacement speed during the loading and unloading half-cycles.

III. Results

(1) Indentation Stress–Strain Curves

Figure 1 plots indentation stress–strain data for the AF, PA, and OA Mg-PSZ materials. The dashed line is the Hertzian relation $p_0 = (3E/4\pi k)a/r$ for purely elastic contacts, using Young's modulus $E = 210$ GPa for Mg-PSZ and coefficient $k = 0.69$ for WC spheres on Mg-PSZ.[13,26] The solid curves through the data are empirical fits. For all three materials, the measured curve bends away from the ideal elastic behavior at low strain, confirming a plastic component in the deformation. This plastic component increases with the aging time, i.e., in the order AF → PA → OA.

(2) Optical Microscopy

Micrographs of the surface damage obtained at radius $r = 3.18$ mm and peak load $P = 1000$ N are shown for each of the AF, PA, and OA materials in Fig. 2. The contact pressures for these three materials are $p_0 = 5.4$, 4.9, and 4.3 GPa, respectively, i.e., in an intermediate region of Fig. 1. The impression becomes more pronounced in the order AF → PA → OA, consistent with the trend to increasing plasticity in Fig. 1. Clear differences in the qualitative features are apparent in the three surface patterns:

(a) In AF there is little sign of a residual depression at the contact center, but very faint traces of incipient cone cracks (arrows) appear at the contact periphery.

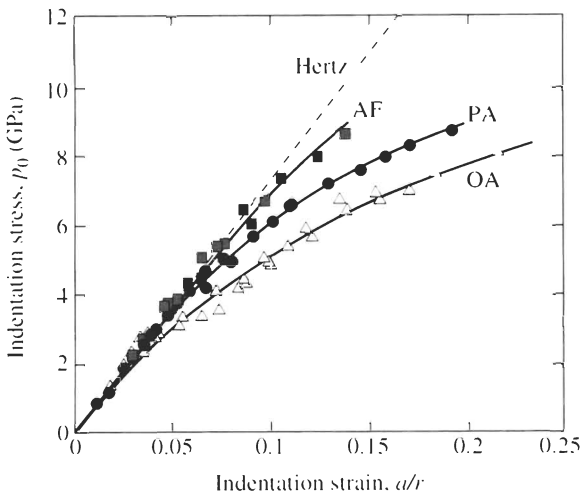

Fig. 1. Indentation stress–strain curves for eutectic-aged Mg-PSZ, using WC spheres of radii $r = 1.59$, 1.98, 3.18, 4.76, 7.94, and 12.70 mm (not distinguished on data points). Data for as-fired (AF), peak-aged (PA), and over-aged (OA) states. Solid curves are empirical fits to the data. Inclined dashed line is calculated Hertzian linear elastic response for WC sphere on Mg-PSZ.

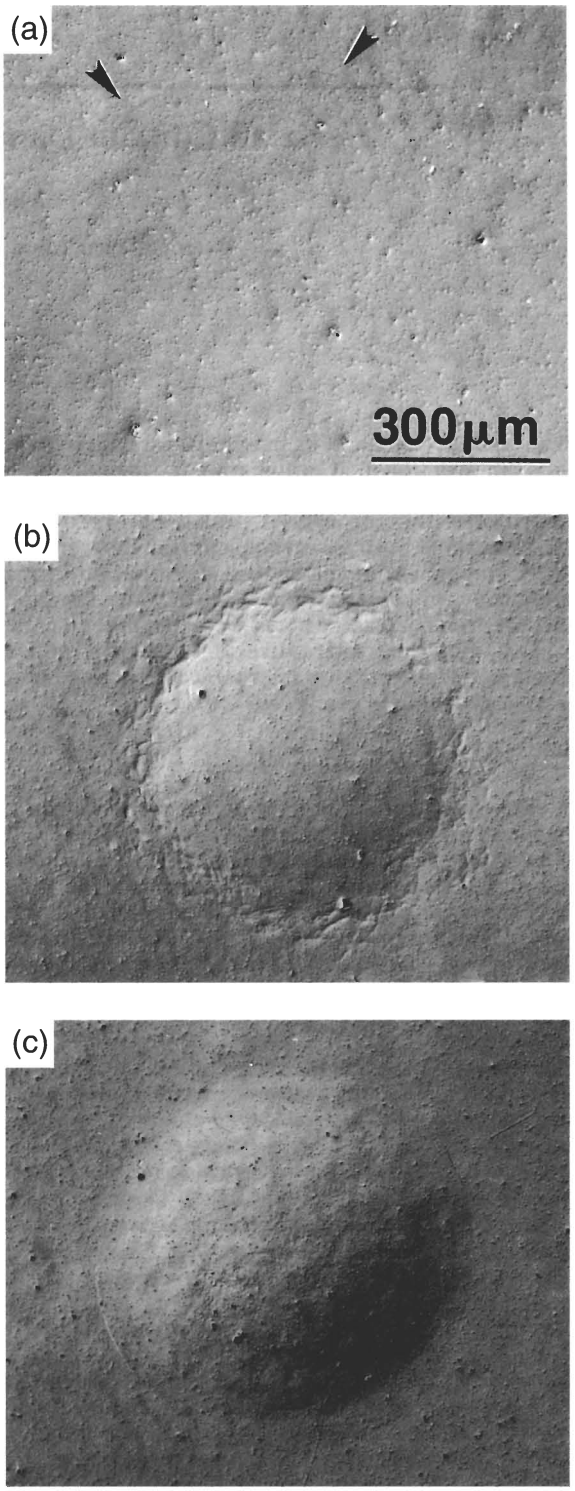

Fig. 2. Surface views of Hertzian damage in Mg-PSZ, for (a) AF, (b) PA, and (c) OA states. Indentations with WC sphere, radius $r = 3.18$ mm, peak load $P = 1000$ N.

(b) In PA the residual impression is smooth over the inner contact, with traces of discrete damage immediately outside. These traces appear to align along shear trajectories, i.e., 45° to radial and hoop directions.[28,29]

(c) In OA the impression is again highly apparent, without peripheral damage but with a recurrence of incipient cone cracks.

Micrographs of the subsurface damage obtained at radius $r = 3.18$ mm and peak load $P = 1000$ N are shown for each of the three materials in the sections of Fig. 3. There is no sign of downward propagating cone cracks, even in the AF and OA

specimens (cf. Figs. 2(a) and (c)). In all three cases the damage is discrete at the grain level and concentrated in the region of high compression–shear stress below the contact:

(a) In AF grain boundary microcracking is visible, similar to that seen in brittle polycrystalline ceramics like alumina[13,19] and silicon nitride.[22] However, unlike these other ceramics, there is no discernible sign of any precursor intragranular deformation.

(b) In PA the damage is characterized by a significant surface rumpling, with *t–m* transformation bands across individual grains.[12,29,30] Again (cf. Fig. 2(b)), there appears to be a tendency for the deformation to align along shear trajectories.[28,29]

(c) In OA the damage appears to be relatively modest, contrary to what might be anticipated from the observed deep impression in Fig. 2(c). There is some surface roughness, but on a much reduced scale relative to PA (Fig. 3(b)), and no bands are seen within individual grains. Some grain boundary microcracking is evident, as in AF (Fig. 3(a)), but again on a much reduced scale.

(3) Acoustic Emission

Plots of cumulative acoustic energy as a function of contact time during an indentation cycle at sphere radius r = 3.18 mm and peak load P = 1500 N are shown for the AF, PA, and OA materials in Fig. 4. In all three materials the acoustic activity occurs almost exclusively during the loading half-cycle. The acoustic activity is relatively intense in AF, modest in OA, and barely detectable in PA. This trend correlates with the degree of microcracking observed in Fig. 3.

IV. Discussion

We have used Hertzian indentation to investigate the mechanical response of a Mg-PSZ ceramic in three stages of heat treatment: as-fired (AF), peak-aged (PA), and over-aged (OA). Indentation stress–strain curves (Fig. 1) demonstrate a significant plastic component in the deformation response, increasing in the order AF → PA → OA. This differs from the reported trend in traditional toughness and strength studies, where optimal properties are observed in the PA state.[4] As far as impact energy absorbing capacity is concerned, it is the OA state which is optimal.

Micrographic examination of the surface (Fig. 2) and subsurface (Fig. 3) contact regions reveals the nature of the damage. Propagation of macroscopic cone cracks, the traditional response for homogeneous brittle solids, is suppressed. This suppression is attributable to an intergranular mode of fracture in the Mg-PSZ, as well as to the relaxation of tensile stresses from the onset of "plasticity" (below). Downward deflection of any incipient surface rings (Figs. 2(a) and 2(c)) along weak grain boundaries diverts the crack front away from the tensile stress trajectories into a compressive field.[15] In this context we recall the moderately large grain size, 35 μm, in the present Mg-PSZ, so the deflections are not insignificant relative to the scale of the contact radius (≈250 μm, Fig. 2). As has been well documented for alumina,[19] the suppression of cone fracture is dramatically more pronounced at larger grain sizes.

In all three aging states the plastic deformation is accommodated as distributed grain-localized damage within the confined compression–shear contact zone below the contact, similar to that observed in other heterogeneous ceramics.[14,19–23] However, the nature of the damage appears to be fundamentally different in each material. In zirconia, the *t–m* transformation is a well-established plasticity mechanism.[1,2,31,32] In the present Mg-PSZ,

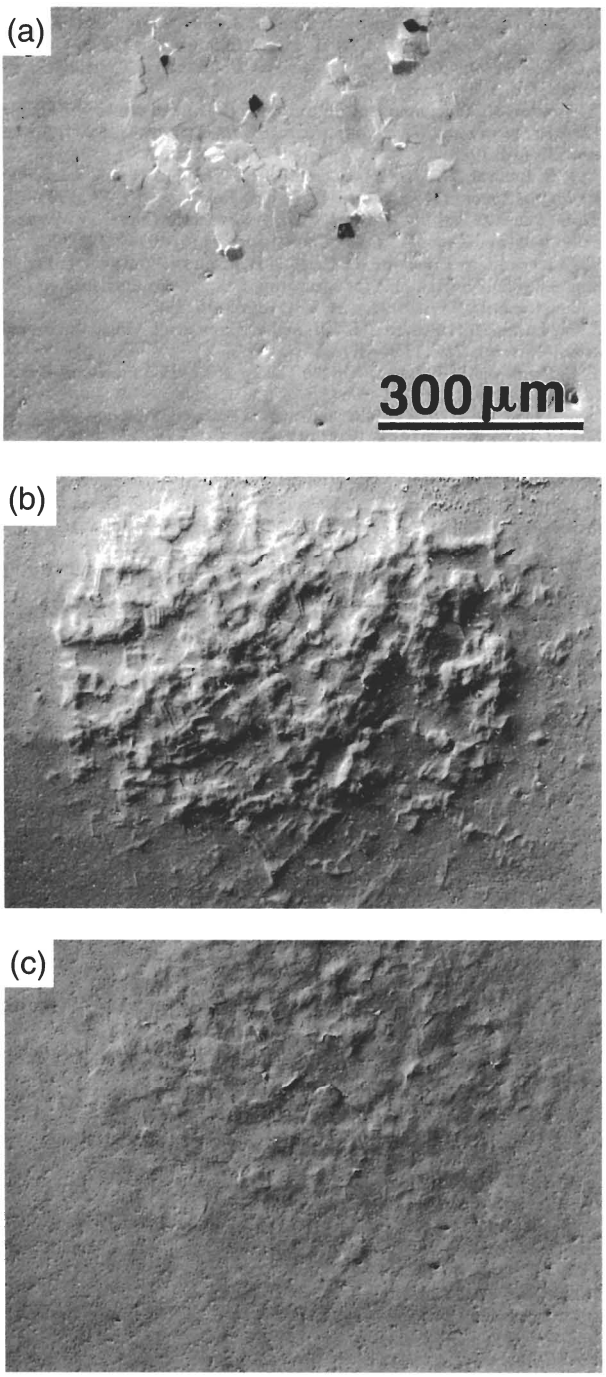

Fig. 3. Subsurface views of Hertzian damage in Mg-PSZ, for (a) AF, (b) PA, and (c) OA states, obtained using bonded-interface section technique. Indentations with WC sphere, radius r = 3.18 mm, peak load P = 1000 N.

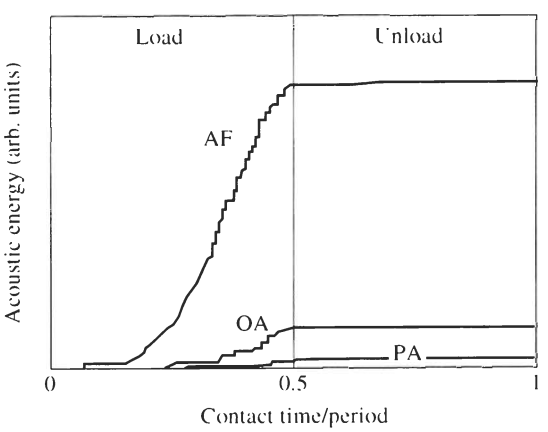

Fig. 4. Cumulative acoustic energy versus normalized contact time during load–unload indentation cycle at constant crosshead speed in AF, PA, and OA Mg-PSZ specimens, using WC sphere of radius r = 3.18 mm at peak load P = 1500 N.

this mechanism appears to play a significant role only in the PA state, as characteristic surface rumpling and shear bands within grains in Fig. 3(b).[2,12,29] Recalling that the contact deformation occurs in a region of strong hydrostatic compression, we conclude that it is solely the shear component of the field that is responsible for activating the transformation in this instance.[8] Once transformation does occur, expansion of the precipitates must inevitably augment the existing state of hydrostatic compression within the subsurface zone, helping to suppress any tendency to microcracking. This is consistent with the almost total absence of acoustic emission for the PA material in Fig. 4.

In the AF state, considerable microcracking is observed at the grain boundaries within the subsurface damage zone, Fig. 3(a). Generation of this kind of facet-scale microcracking is often the consequence of some precursor shear fault, e.g., twinning in alumina,[13] crystallographic slip in silicon nitride.[22] Such intragranular shear faults provide intense local tensile stress concentrations at the weak grain boundaries, and thereby overcome the inhibiting influence of the compressive contact stresses. They also account for any indentation plasticity. No such faults were evident in the AF material in the present observations, even at higher resolution in the scanning electron microscope. This lack of conspicuous faulting is not inconsistent with the relatively small deviation of the AF indentation stress–strain curve from the ideal linear elasticity in Fig. 1. Moreover, in some materials with especially weak boundaries, e.g., machinable mica-containing glass-ceramics[20] and silicon carbide platelet composites,[23] microcracking can occur by interboundary sliding without precursor deformation. The high density of subsurface microcracking in Fig. 3(a) correlates with the relatively high level of AF acoustic emission in Fig. 4. We note that the bulk of the acoustic activity, and hence microcrack *initiation*, occurs during the loading half-cycle. However, this does not exclude the possibility that the bulk of microcrack *propagation* might actually occur during unloading, as the stabilizing influence of the compressive contact field is progressively released.[33]

In the OA state, virtually all of the precipitates already exist in the monoclinic phase prior to indentation, so transformation is no longer so effective. Thus, the extreme surface rumpling and shear banding that characterize PA in Fig. 3(b) are not so apparent in Fig. 3(c). Yet OA shows a substantially greater deviation than PA from a linear elastic stress–strain response in Fig. 1. Hence there must exist some other, even more effective mechanism of plasticity associated with the post-transformation state in the Mg-PSZ. This mechanism is attributable to low-stress monoclinic twinning within the submicroscopic monoclinic precipitates.[31,34] Twinning can produce highly localized, submicroscopic cracking at the interphase boundaries,[31] which can further increase the plastic compliance. Twinning is also unlikely to be as effective as transformation in inhibiting larger-scale grain-facet fracture, consistent with the recurrence of modest grain facet microcracking in Fig. 3(c) and OA acoustic emission in Fig. 4. Finally, twinning in the OA state would not be expected to produce as strong an uplift on the section face as transformation in the PA state, consistent with the relatively smooth damage pattern in Fig. 3(c) (cf. Fig. 3(b)).

The observations in this work raise issues concerning deformation and fracture processes in zirconia ceramics. Transformation is an important element of the damage characterization, but other modes exist, and can be even more effective in accommodating strain. Microcracking is an important element of these other modes, and could account for diminished wear resistance in the AF and OA states.[35] The Hertzian test presents itself as a particularly simple route to investigate such damage, and is readily extendable to cyclic loading.[13] A more detailed study of these considerations in Mg-PSZ will be presented elsewhere.

Acknowledgments: We acknowledge valuable discussions with D. B. Marshall, N. P. Padture, and A. H. Heuer.

References

[1]R. C. Garvie, R. H. J. Hannink, and R. T. Pascoe, "Ceramic Steel?," *Nature (London)*, **258**, 703 (1975).

[2]D. J. Green, R. H. J. Hannink, and M. V. Swain, *Transformation Toughening of Ceramics*. CRC Press, Boca Raton, FL, 1989.

[3]R. H. J. Hannink and M. V. Swain, "Progress in Transformation Toughening of Ceramics," *Annu. Rev. Mater. Sci.*, **24**, 359–408 (1994).

[4]S. Lathabai and R. H. J. Hannink, "Microstructure–Crack Resistance–Fatigue Correlations in Eutectoid-Aged Mg-PSZ"; pp. 360–70 in *Science and Technology of Zirconia V*. Edited by S. P. S. Badwal, M. J. Bannister, and R. H. J. Hannink. Technomic Publishing Co., Lancaster, PA, 1993.

[5]P. Chantikul, S. J. Bennison, and B. R. Lawn, "Role of Grain Size in the Strength and *R*-Curve Properties of Alumina," *J. Am. Ceram. Soc.*, **73** [8] 2419–27 (1990).

[6]S.-J. Cho, B. J. Hockey, B. R. Lawn, and S. J. Bennison, "Grain-Size and *R*-Curve Effects in the Abrasive Wear of Alumina," *J. Am. Ceram. Soc.*, **72** [7] 1249–52 (1989).

[7]S.-J. Cho, H. Moon, B. J. Hockey, and S. M. Hsu, "The Transition from Mild to Severe Wear in Alumina During Sliding," *Acta Metall.*, **40** [1] 185–92 (1992).

[8]A. H. Heuer and L. W. Hobbs (Eds.), Advances in Ceramics, Vol. 3, *Science and Technology of Zirconia*. American Ceramic Society, Columbus, OH, 1981.

[9]N. Claussen, M. Rühle, and A. H. Heuer (Eds.), Advances in Ceramics, Vol. 12, *Science and Technology of Zirconia II*. American Ceramic Society, Columbus, OH, 1984.

[10]S. Somiya, N. Yamamoto, and H. Yanagida (Eds.), Advances in Ceramics, Vol. 24A,B, *Science and Technology of Zirconia III*. American Ceramic Society, Westerville, OH, 1988.

[11]S. P. S. Badwal, M. J. Bannister, and R. H. J. Hannink (Eds.), *Science and Technology of Zirconia V*. Technomic Publishing Co., Lancaster, PA, 1993.

[12]D. B. Marshall and M. V. Swain, "Crack-Resistance Curves in Magnesia-Partially-Stabilized Zirconia," *J. Am. Ceram. Soc.*, **71** [6] 399–407 (1988).

[13]F. Guiberteau, N. P. Padture, H. Cai, and B. R. Lawn, "Indentation Fatigue: A Simple Cyclic Hertzian Test for Measuring Damage Accumulation in Polycrystalline Ceramics," *Philos. Mag. A*, **68** [5] 1003–16 (1993).

[14]B. R. Lawn, N. P. Padture, H. Cai, and F. Guiberteau, "Making Ceramics 'Ductile,' " *Science*, **263**, 1114–16 (1994).

[15]F. C. Frank and B. R. Lawn, "On the Theory of Hertzian Fracture," *Proc. R. Soc. London*, **A299** [1458] 291–306 (1967).

[16]B. R. Lawn and T. R. Wilshaw, "Indentation Fracture: Principles and Applications," *J. Mater. Sci.*, **10** [6] 1049–81 (1975).

[17]A. G. Evans and T. R. Wilshaw, "Quasi-Plastic Solid Particle Damage in Brittle Materials," *Acta Metall.*, **24**, 939–56 (1976).

[18]K. Zeng, K. Breder, and D. J. Rowcliffe, "The Hertzian Stress Field and Formation of Cone Cracks: II. Determination of Fracture Toughness," *Acta Metall.*, **40** [10] 2601–605 (1992).

[19]F. Guiberteau, N. P. Padture, and B. R. Lawn, "Effect of Grain Size on Hertzian Contact in Alumina," *J. Am. Ceram. Soc.*, **77** [7] 1825–31 (1994).

[20]H. Cai, M. A. S. Kalceff, and B. R. Lawn, "Deformation and Fracture of Mica-Containing Glass-Ceramics in Hertzian Contacts," *J. Mater. Res.*, **9** [3] 762–70 (1994).

[21]H. Cai, M. A. S. Kalceff, B. M. Hooks, B. R. Lawn, and K. Chyung, "Cyclic Fatigue of a Mica-Containing Glass-Ceramic at Hertzian Contacts," *J. Mater. Res.*, **9** [10] 2654–61 (1994).

[22]H. H. K. Xu, L. Wei, N. P. Padture, B. R. Lawn, and R. L. Yeckley, "Effect of Microstructural Coarsening on Hertzian Contact Damage in Silicon Nitride," *J. Mater. Sci.*, in press.

[23]N. P. Padture and B. R. Lawn, "Toughness Properties of a Silicon Carbide with an *In-Situ* Induced Heterogeneous Grain Structure," *J. Am. Ceram. Soc.*, **77** [10] 2518–22 (1994).

[24]T. O. Mulhearn, "The Deformation of Metals by Vickers-Type Pyramidal Indenters," *J. Mech. Phys. Solids*, **7**, 85–96 (1959).

[25]D. Tabor, *Hardness of Metals*. Clarendon, Oxford, U.K., 1951.

[26]M. V. Swain and B. R. Lawn, "A Study of Dislocation Arrays at Spherical Indentations in LiF as a Function of Indentation Stress and Strain," *Phys. Status Solidi*, **35** [2] 909–23 (1969).

[27]M. V. Swain and J. T. Hagan, "Indentation Plasticity and the Ensuing Fracture of Glass," *J. Phys. D*, **9**, 2201–14 (1976).

[28]J. T. Hagan and M. V. Swain, "The Origin of Median and Lateral Cracks at Plastic Indents in Brittle Materials," *J. Phys. D*, **11** [15] 2091–102 (1978).

[29]R. H. J. Hannink and M. V. Swain, "A Mode of Deformation in Partially Stabilized Zirconia," *J. Mater. Sci.*, **16**, 1428–31 (1981).

[30]J. Lankford, "Plastic Deformation of Partially Stabilized Zirconia," *J. Am. Ceram. Soc.*, **66** [11] C-212–C-213 (1983).

[31]B. C. Muddle and P. M. Kelly, "Stress-Activated Martensitic Transformation and Transformation Plasticity," *Mater. Forum*, **11**, 182–93 (1988).

[32]V. Tikare and A. H. Heuer, "Temperature-Dependent Indentation Behavior of Transformation-Toughened Zirconia-Based Ceramics," *J. Am. Ceram. Soc.*, **74** [3] 593–97 (1991).

[33]B. R. Lawn, N. P. Padture, F. Guiberteau, and H. Cai, "A Model for Microcrack Initiation and Propagation Beneath Hertzian Contacts in Polycrystalline Ceramics," *Acta Metall.*, **42** [5] 1683–93 (1994).

[34]I-W. Chen, "Implications of Transformation Plasticity in ZrO_2-Containing Ceramics: II, Elastic-Plastic Indentation," *J. Am. Ceram. Soc.*, **69** [3] 189–94 (1986).

[35]S. Lathabai; unpublished work. □